Scanned for the Undersea and Hyperbaric Medical Society by The Rubicon Foundation
in cooperation with Global Underwater Explorers. (http://rubicon-foundation.org)

Undersea & Hyperbaric Medicine, Vol. 22, No. 4, 1995

Effect of SF_6–O_2 (80/20) breathing on air bubbles in rat tissues

O. HYLDEGAARD and J. MADSEN

Department of Medical Physiology, The Panum Institute, University of Copenhagen, Denmark

Hyldegaard O, Madsen J. Effect of SF_6–O_2 (80/20) breathing on air bubbles in rat tissues. Undersea Hyperbaric Med 1995; 22(4):355–365.—We studied the effect of SF_6–O_2 breathing on air bubbles injected into skeletal muscle, rat-tail tendon, the anterior chamber of the eye, and spinal white matter. Decompression-induced nitrogen bubbles in adipose tissue were studied during breathing of SF_6–O_2 (80/20). The results of SF_6–O_2 breathing are compared with previous experiments using heliox (80/20) as the breathing medium. Bubbles studied in skeletal muscle, eye chamber, and spinal white matter were found to behave in a two-phased manner during SF_6–O_2 (80/20) breathing. All bubbles would initially decrease rapidly in size for a period of 10–80 min (depending on the tissue). Subsequently, the bubbles stabilized and decreased in size with a shrinking rate near zero. In spinal white matter, very small bubbles could disappear before development of the slow phase. All bubbles in tendon shrank at a rather constant rate during SF_6–O_2 (80/20) breathing until they disappeared. During SF_6–O_2 (80/20) breathing, all bubbles in adipose tissue shrank and disappeared at least as fast as during heliox (80/20) breathing. Just before disappearance of the bubbles the shrinking rate slowed. Comparison of the effects of SF_6–O_2 (80/20) and heliox (80/20) breathing suggests that coun-tercurrent gas exchange is at work in some tissues.

spinal white matter, bubbles, adipose tissue, perfusion limitation, eye, diffusion limitation, tendon, countercurrent, muscle

SF_6 is a biologically inactive gas characterized by a very low solubility coefficient in blood and water (Table 1), lower than that of nitrogen, helium and oxygen. Because of its large molecular weight (MW = 146) the diffusion coefficient is smaller than that of N_2, He, and O_2 (Table 1) (1). Breathing SF_6–O_2 might therefore be beneficial in the treatment of decompression sickness (DCS) with symptoms from the joints (i.e., bends) where bubbles have been found to form in aqueous tissues such as ligament and tendon (2,3). The ratio between the solubility of SF_6 in lipid and blood (i.e., the partition coefficient, λ) is 7 times greater than that of N_2 (Table 1) (4). Consequently, if gas exchange is limited by the perfusion rate, a tissue consisting of lipid will eliminate the N_2 surplus 7 times faster than it will saturate with SF_6 after a change of N_2 to SF_6 in the breathing mixture.

Table 1: Physical Properties of Inert Gases

	Ostwald Solubility Coefficients at 37°C, ml gas 37°C × ml Fluid^{-1}				Diffusion Coefficients, × 10^{-6} cm^2 × s^{-1}		Solubility Coefficients × Diffusion Coefficients, × 10^{-6} cm^2 × s^{-1}		Partition Coefficient λ	
	Oil[a]	Water[a]	Lipid[b], 85%	Blood[a]	Oil	Water	Oil	Water	$\lambda \frac{\alpha_{tissue,lip.}}{\alpha_{blood}}$	$\lambda \frac{\alpha_{H_2O}}{\alpha_{blood}}$
Nitrogen MW = 28.01	0.0745	0.0143	0.066	0.0148	7.04[c]	30.1[c]	0.525	0.430	4.46	0.966
Helium MW = 4	0.0168	0.0098	0.016	0.0094	18.6[c]	63.2[c]	0.312	0.619	1.70	1.043
Oxygen MW = 32	0.133	0.0271	0.117	0.0261	6.59[c]	28.2[c]	0.876	0.764	4.48	1.038
SF_6, MW = 146	0.277	0.0041	0.236	0.0074	3.08[d]	13.18[d]	0.853	0.054	31.89	0.554

[a]Averages from values cited from (1); a very low value for the solubility of nitrogen in oil obtained with outdated technique has been omitted. [b]Calculated as weighted averages of oil and water values, disregarding possible salt effects. [c]From (1). [d]Calculated from nitrogen data by Grahams law.

Scanned for the Undersea and Hyperbaric Medical Society by The Rubicon Foundation in cooperation with Global Underwater Explorers. (http://rubicon-foundation.org)

Scanned for the Undersea and Hyperbaric Medical Society by The Rubicon Foundation
in cooperation with Global Underwater Explorers. (http://rubicon-foundation.org)

Therefore, and because of its smaller solubility in blood, breathing SF_6–O_2 should also promote shrinking and disappearance of bubbles in lipid tissues if used as a breathing medium after an air dive. However, in a lipid tissue the diffusibility (i.e., the product of diffusion coefficient and solubility coefficient) of SF_6 is 1.6 times greater than that of N_2. Thus, if gas exchange between blood and bubbles in a lipid tissue is limited mainly by extravascular diffusion, a N_2 bubble should grow after a shift from air to SF_6–O_2 breathing. The purpose of the present experiments was to examine in aqueous and lipid tissues the behavior of N_2 bubbles during breathing of SF_6–O_2 (20% O_2 in 80% SF_6) as compared to the effect of heliox (20% O_2 in 80% He) breathing described in previous papers (5–7).

METHODS

Female rats weighing 250–350 g were anesthetized with sodium thiomebumal (0.1 g/kg) intraperitoneally. Cannulation of trachea, blood pressure recording, and temperature regulation and recording were all performed as described in previous papers (5–7). The animals were placed in the pressure chamber and exposed to increased ambient pressure, according to the different pressure profiles described below. Bubbles were made either by decompression (adipose tissue) or by micro injection of air as described below. The observed bubble field was illuminated by two flexible fiber optics and studied at ×40 magnification through a Wild M-10 stereo microscope fitted with a color video camera. The image was continuously monitored and recorded on videotape. With a frame grabber board, real-time images could be grabbed to a Macintosh IISi computer and measurements of bubble size made at any time. In the experiments with bubbles studied in muscle or tendon, all animals initially breathed air in the observation period. After some 20–80 min, the breathing gas would be changed from air to SF_6–O_2. In the adipose tissue and spinal white matter experiments the breathing gas would be SF_6–O_2 from the beginning of the observation period. Through a T-connection on the tracheal tube, the breathing gas was flowing at a constant rate of 1.5–2.0 liters/min. All observations were made at atmospheric pressure.

At the end of the observation period the abdomen and thorax were opened and the animals were examined under the microscope for intra- or extravascular gas formation before exsanguination.

Muscle and tendon: The musculus obliquus externus or the adductors of the thigh were exposed through skin incisions. The tendons of the tail were exposed through a 3-cm longitudinal and two 1-cm transverse skin incisions. The exposed tissue areas in muscle were then covered with gas-impermeable mylar and a 12.5-μm-thick polyethylene membrane to prevent evaporation during exposure in the pressure chamber. In tendon, a glass cover was used with the polyethylene membrane.

Just after the pressure exposure in the chamber the mylar, glass, and plastic covers were removed and a bubble of about 1–1.5 μl of air was injected superficially into the muscle. In the rat-tail tendon, air bubbles of 0.5–1.0 μl were injected. The injection technique has been described previously (7). The bubbles were covered with mylar (i.e., in muscle) or glass (i.e., in tendon) and all exposed tissue covered with a polyethylene membrane. In some experiments a thermoprobe was placed under the plastic film to check the temperature of the exposed tissue.

Eye: The rats were placed on their right side with the head elevated and turned so the circumference of the left cornea was in a horizontal plane. After dilating the iris with atropine, an air bubble of 0.1–0.5 μl was injected into the anterior chamber and a 1.0-mm-thick glass contact lens placed on the eye to prevent gas exchange with the surrounding room air (7).

Scanned for the Undersea and Hyperbaric Medical Society by The Rubicon Foundation
in cooperation with Global Underwater Explorers. (http://rubicon-foundation.org)

Adipose tissue: After the pressure exposure, the animal was removed from the pressure chamber and the abdomen opened in the midline exposing the abdominal adipose tissue. In the adipose tissue, two or three widely separated bubbles partly covered with adipocytes were selected for study in each rat. The bubbles were covered with gas-impermeable mylar and all exposed tissue with a polyethylene membrane; the animal was then placed under the microscope. The experimental set-up and methods are otherwise similar to the procedures described in our previous paper (5).

Spinal white matter: In anesthetized rats the cervical spinal cord between C1 and C2 was exposed leaving the dura intact as described in (6). To examine the effect of initial bubble size on the volume change during SF_6–O_2 breathing, the rats were assigned to one of two groups, experiments A and B.

Experiment A: After exposing the cervical medulla, the incision was closed and the rat exposed to pressure. The animal was removed from the chamber and placed under the heating lamp. The incision was reopened and the dura removed exposing the cervical medulla. An air bubble of 1–1.5 μl was injected superficially into the posterior funiculus. The bubble was covered with a piece of gas-impermeable glass. Two control experiments using heliox breathing showed that glass-covered bubbles disappeared at similar rates as previously reported (6) in which the bubbles were not protected by glass from the surrounding room air.

Experiment B: Two to three bubbles of approximately 0.1–0.2 μl were injected into the posterior funiculus of the spinal white matter. If the visible area of the injected bubble was larger than 0.05 mm^2 the rat was left breathing air for 20–40 min, during which period the bubbles decreased in size to a visible surface area of less than 0.05 mm^2. From this point of the observation period, the bubbles were studied either during continued air breathing or while breathing SF_6–O_2. No animal in experiment B was exposed to increased ambient pressures since the waiting period needed for the bubbles to reduce to less than 0.05 mm^2 would make the animals incomparable with respect to supersaturation.

Pressure exposures: In the muscle and tendon experiments the animals were exposed to a pressure of 3.5 atm abs (355 kPa) for 1 h and decompressed over 7.5 min with short stops at 3.0, 2.0, and 1.5 atm abs (7). In the spinal white matter studies (experiment A) animals were exposed to 3.1 atm abs (314 kPa) for 4 h and decompressed over 20 min in three stages (6). In the experiments with adipose tissue the animals were exposed to 3.3 atm abs (334 kPa) for 4 h and decompressed over 20 min in three stages (5). In the eye experiments the animals were not exposed to increased ambient pressures.

Breathing gas mixture: Pure SF_6 was mixed through a flowmeter with O_2 into a 200-liter gas-impermeable Douglas plastic bag at normobaric conditions. The mixture of SF_6–O_2 in the Douglas plastic bag was analyzed for O_2 in an ABL 30 radiometer blood–gas analyzer and adjusted until a final mixture of 20% O_2 in 80% SF_6 was obtained.

Evaluation of bubbles: Bubbles injected into rat-tail tendon, muscle, or spinal white matter may be irregular in shape (6,7). Therefore, we assess their size by the bubble area visible on the microscopic image using automated planimetry. Since decompression-induced bubbles in rat adipose tissue as well as bubbles injected into the eye chamber are spherical, bubble diameters can be measured and volumes calculated.

Data analysis and statistics: To examine whether the difference between two mean values of calculated bubble shrinking rate was different from zero, analysis of variance (ANOVA) was performed on the difference between mean values in the different treatment groups (8–10). Bubble shrinking rates in tendon were expressed as the mean shrinking rate in square millimeters per minute (slope of a line from first observation after gas shift to last observation or disappearance of bubbles). Average values of bubble shrinking rates

Scanned for the Undersea and Hyperbaric Medical Society by The Rubicon Foundation
in cooperation with Global Underwater Explorers. (http://rubicon-foundation.org)

are given ±SEM. Bubble shrinking rates in adipose tissue were expressed as the mean shrinking rate in nanoliters per minute (±SEM). When multiple bubbles were studied in one animal, the mean value was used in the statistical comparison. $P < 0.05$ is regarded as the limit for significance.

RESULTS

General condition of animals: The animals were observed for up to 305 min post-decompression. Regardless of the pressure exposure, the animals remained in good shape as evaluated by mean arterial blood pressure (MAP) and respiration. During the muscle and tendon experiments, one rat died of DCS, with ample bubbles present in the veins. In the eye experiments, animals remained unaffected as evaluated by MAP and respiration.

Mean arterial blood pressure: Before and during the 1 or 4 h air breathing under pressure, MAP was in the range of 120–160 mmHg. When animals were decompressed it fell to a level of 80–140 mmHg. During subsequent SF_6–O_2 breathing, blood pressure was in the range of 80–160 mmHg. In the undived animals, MAP was in the range of 100–160 mmHg.

State of tissue: In muscle during the observation period, perfusion in the small vessels with a diameter of approximately 10–15 μm was clearly visible and appeared unaffected throughout the experiment. The tissue temperature varied between 36.5° and 39.8°C depending on the switching on and off of the heating lamp. Occasionally, small muscle fiber twitches could be observed.

In tendon during the experiments, perfusion in the smaller vessels (i.e., 10–15 μm) was clearly visible. Some bleeding of the skin could be seen when this was split from the tendons during the preparation phase. The temperature of the tissue varied between 34.9° and 37.0°C.

In neither muscle nor tendon experiments were intra- or extravascular bubbles observed at the end of the experiment.

During the entire observation period the iris remained in its dilated state, and the blood flow in the vessels of the iris was clearly visible at all times.

In adipose tissue, perfusion in the smaller and larger vessels was visible throughout the experiment until the animals were killed. The temperature at the surface of the tissue varied between 36° and 39°C. Only extravascular bubbles were observed after decompression.

In the observation period during experiment A, perfusion in the larger pial vessels was clearly visible at all times whereas the circulation in the smallest vessels close to the bubble was impeded. The temperature at the surface of the tissue varied between 36.5° and 39.7°C. No intra- or extravascular bubbles were observed on examination at the end of the experiment.

In experiment B (i.e., no pressure exposure, small bubbles) perfusion in the larger and smaller pial vessels was clearly visible at all times.

Effects of SF_6–O_2 breathing on bubbles: During breathing of SF_6–O_2 in muscle ($n = 6$), eye ($n = 6$), adipose tissue ($n = 13$), and spinal white matter (experiment A, $n = 5$) all bubbles shrank in a biphasic manner. Initially they shrank fast, but after some time (10–60 min depending on the tissue) the shrinking rate slowed to a rate approaching zero. During breathing of SF_6–O_2 in experiment B, most bubbles ($n = 13$) shrank and disappeared faster than during air breathing ($n = 14$). In tendon ($n = 11$), bubbles shrank consistently until they disappeared from view. All bubbles in adipose tissue disappeared from view in the observation period. The results are depicted in Figs. 1–7 and discussed below.

Scanned for the Undersea and Hyperbaric Medical Society by The Rubicon Foundation
in cooperation with Global Underwater Explorers. (http://rubicon-foundation.org)

DISCUSSION

Bubbles in muscle behave very differently during breathing of SF_6–O_2 (Fig. 1) and heliox (7). Although they shrink at a constant rate and disappear quickly during heliox breathing, their shrinking rate during SF_6–O_2 breathing is biphasic; initially fast, then very slow. The first phase reflects the disappearance of N_2 from the bubble. When the bubble only contains SF_6 the disappearance rate is expected to be slow because the driving force is small (i.e., the O_2 window), the solubility of SF_6 in blood low, and the surrounding aqueous tissue presumably saturated with SF_6. Lack of a slow phase in the heliox experiments (7) suggests a role of the countercurrent mechanism demonstrated in skeletal muscle by Sejrsen et al. (11–13), Piiper and Mayer (14), and discussed by Homer et al. (15,16). Countercurrent is a mechanism whereby a fast diffusing gas, such as He, is shunted from arteries to veins where arteries and veins lie in intimate contact. Since the diffusibility of He is 11.5 times that of SF_6 in aqueous surroundings (Table 1), it is possible that most of the He is carried away from the tissue because of countercurrent transfer, and that little if any He reaches the bubble. SF_6 transport would be much less affected by the countercurrent mechanism. However, SF_6 may initially diffuse into perivascular adipocytes in which SF_6 is 32 times more soluble than in blood (4). This mechanism has been demonstrated in cat gastrocnemius muscle by Tønnesen and Sejrsen (17) during Xe^{133} blood flow measurements.

In tendon (Fig. 2), SF_6–O_2 breathing consistently caused air bubbles to shrink and disappear. A similar effect is seen during heliox breathing (7) with a tendency for faster shrinking rates. Heliox breathing caused the bubbles to shrink at a mean rate of $67 \cdot 10^{-4}$ $mm^2 \cdot min^{-1}$ (SEM: $\pm 15 \cdot 10^{-4}$ $mm^2 \cdot min^{-1}$) (7) as opposed to $35 \cdot 10^{-4}$ $mm^2 \cdot min^{-1}$ (SEM: $\pm 6 \cdot 10^{-4}$ $mm^2 \cdot min^{-1}$) during SF_6–O_2 breathing ($0.1 > P > 0.05$). The two groups did not differ significantly from each other with respect to size of injected bubbles or time intervals from decompression to bubble injection, first observation, and gas shift.

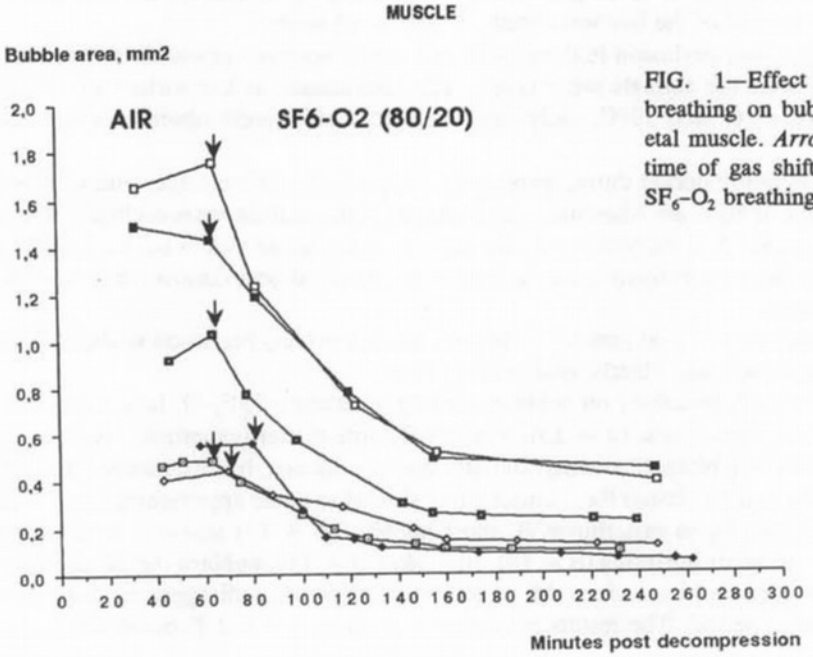

FIG. 1—Effect of SF_6–O_2 breathing on bubbles in skeletal muscle. *Arrows* mark the time of gas shift from air to SF_6–O_2 breathing.

Scanned for the Undersea and Hyperbaric Medical Society by The Rubicon Foundation
in cooperation with Global Underwater Explorers. (http://rubicon-foundation.org)

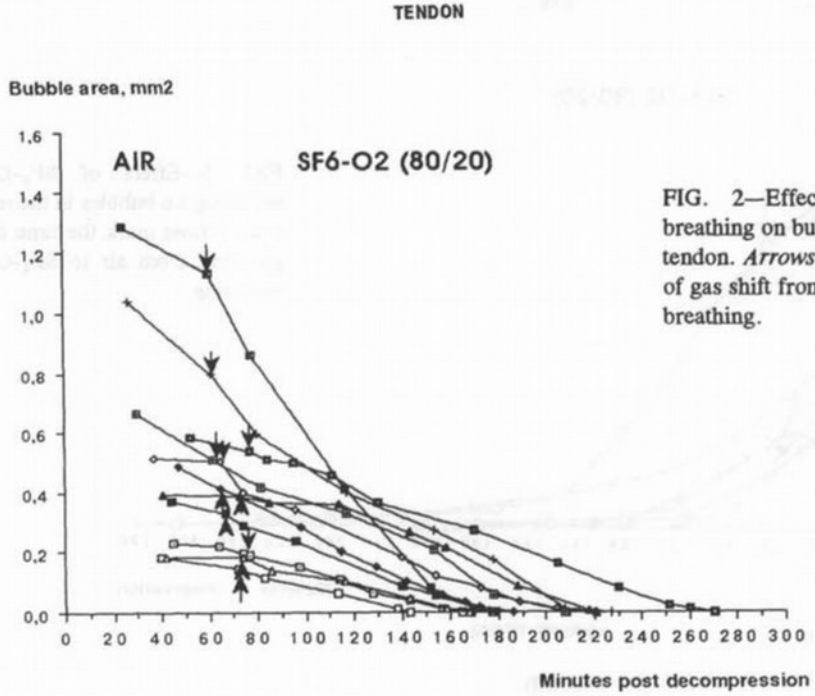

FIG. 2—Effect of SF_6–O_2 breathing on bubbles in rat tail tendon. *Arrows* mark the time of gas shift from air to SF_6–O_2 breathing.

In the tendon experiments there is no slow 2´phase in the disappearance curves. This suggests either that no or very little SF_6 or He ever reaches the bubbles, or that mechanisms additional to removal of He and SF_6 by the blood under influence of the O_2 window are at work. Countercurrent mechanisms may be at work in the long stretch, where arteries and veins lie side by side in the tail. Further, as discussed above, SF_6 may diffuse into perivascular adipocytes before reaching the bubble region. We have observed adipocytes located between the streaks of the tendinous fibers. The tendinous fibers surrounding the bubble are very poorly perfused (18) and thus presumably a very slow tissue. Therefore, diffusion from the bubble to these fibers may accelerate disappearance of the bubble.

In the eye (Fig.3) SF_6-O_2 breathing caused bubbles initially to shrink fast and then very slowly. This is to be expected as SF_6 is 2.3 times less diffusible in water as compared to N_2 and 4.8 times less diffusible than He (Table 1) (4). Thus, the effect of SF_6 in the eye is the opposite from that of He where the bubbles initially grow and then shrink and disappear very fast (7).

In adipose tissue (Fig.4) decompression-induced N_2 bubbles shrank and disappeared during breathing of SF_6–O_2 at approximately the same rate as during breathing of heliox (5). ANOVA between groups showed no significant difference ($P > 0.1$). The faster initial shrinking rate during SF_6–O_2 breathing (1.9 nl · min^{-1}, SEM: ± 0.5 nl · min^{-1}) was not significantly different from that found during heliox breathing (0.5 nl · min^{-1}, SEM: ± 0.1 nl · min^{-1}) ($0.1 > P > 0.05$). This effect of enhanced bubble shrinking rate and disappearance during SF_6–O_2 breathing may be explained by a lower solubility of SF_6 in blood than of N_2 and He (Table 1) and by the 19 times slower tissue saturation with SF_6 (i.e., the higher partition coefficient - λ) as compared to He. Compared to He, SF_6 carried by the blood will distribute itself with much more to be dissolved in the tissue and less to the bubble. Thus, during SF_6 breathing the initial shrinking rate of the bubbles may well be close to the rate at which N_2 is disappearing from the bubbles.

Scanned for the Undersea and Hyperbaric Medical Society by The Rubicon Foundation
in cooperation with Global Underwater Explorers. (http://rubicon-foundation.org)

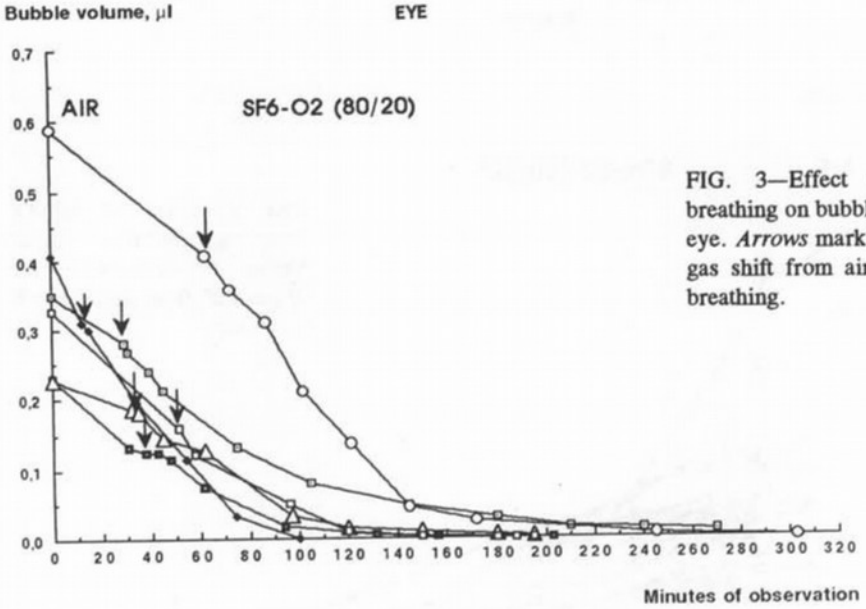

FIG. 3—Effect of SF_6–O_2 breathing on bubbles in the rat eye. *Arrows* mark the time of gas shift from air to SF_6–O_2 breathing.

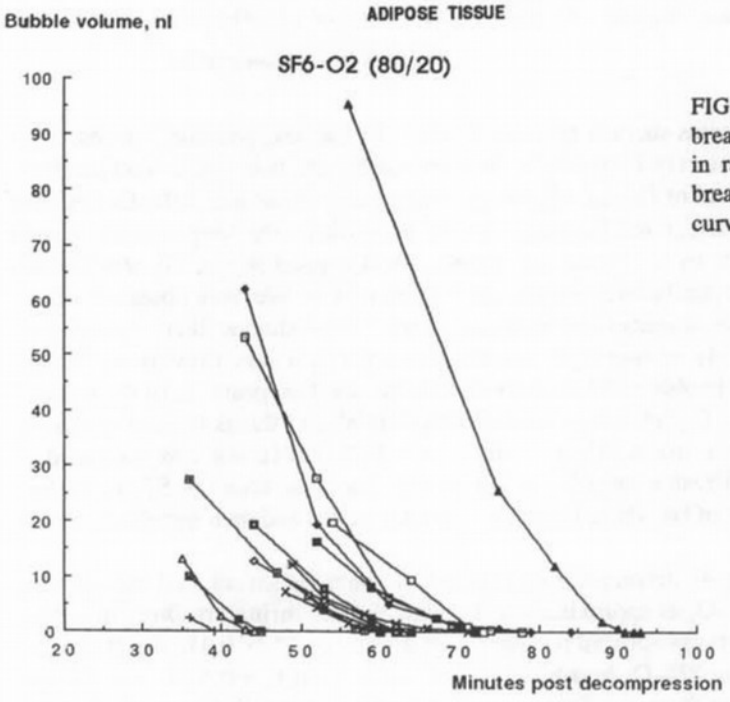

FIG. 4—Effect of SF_6–O_2 breathing on nitrogen bubbles in rat adipose tissue. SF_6–O_2 breathing from first point on curves.

However, just before disappearance, the shrinking rate slowed (Fig.4). This decrease in shrinking rate has not been observed with heliox breathing (5–7) and may be explained by the fact that a certain amount of SF_6 has diffused into the bubble. This final retardation of shrinking is to be expected when the N_2 has disappeared and the bubble consists only of SF_6, which will be removed slowly by the blood under influence of the O_2 window. Thus, larger bubbles in a lipid tissue may initially shrink fast to a smaller size from which they will shrink slowly.

Scanned for the Undersea and Hyperbaric Medical Society by The Rubicon Foundation
in cooperation with Global Underwater Explorers. (http://rubicon-foundation.org)

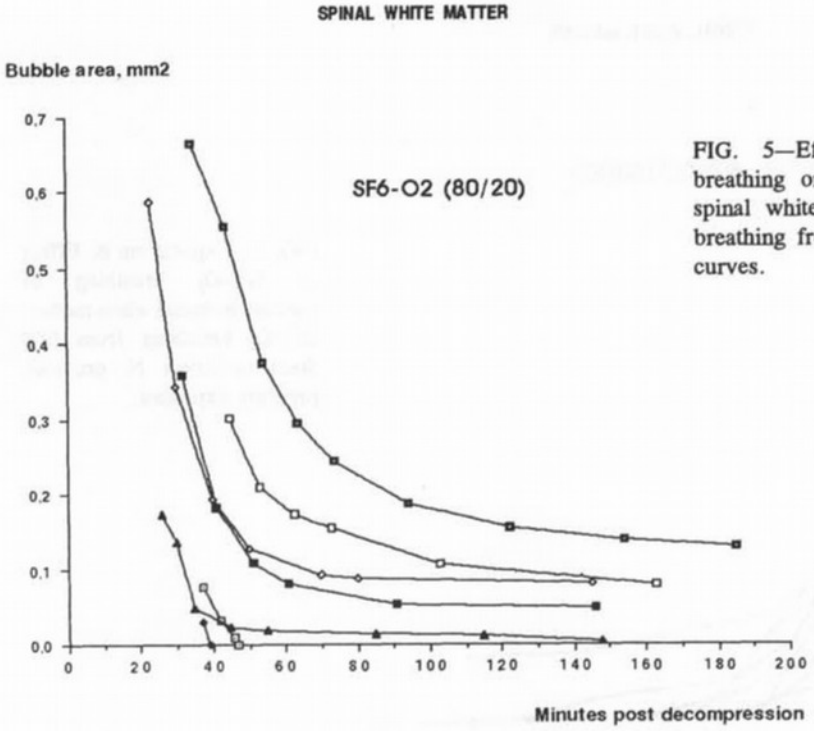

FIG. 5—Effect of SF_6–O_2 breathing on bubbles in rat spinal white matter. SF_6–O_2 breathing from first point on curves.

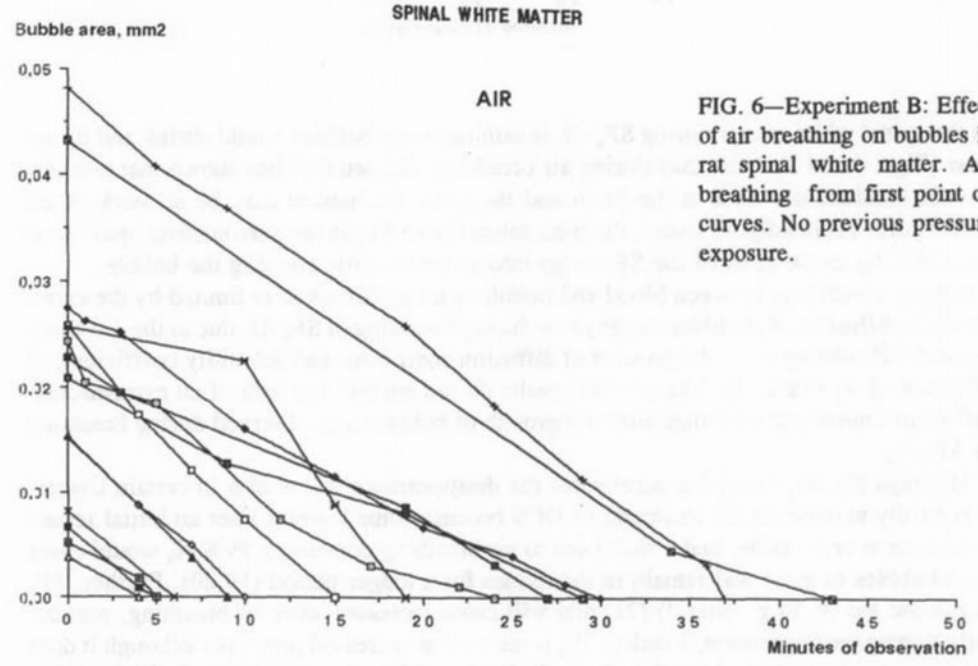

FIG. 6—Experiment B: Effect of air breathing on bubbles in rat spinal white matter. Air breathing from first point on curves. No previous pressure exposure.

In the experiments with injected air bubbles in rat spinal white matter (Fig.5), we observed bubbles to behave in a similar two-phased manner. They would initially shrink fast until they finally slowed and subsequently shrank at a rate slower than during heliox breathing (6). However, two small bubbles were observed to shrink consistently and disappear fast (Fig.5). In experiment B, where injected bubbles of smaller size were studied

Scanned for the Undersea and Hyperbaric Medical Society by The Rubicon Foundation
in cooperation with Global Underwater Explorers. (http://rubicon-foundation.org)

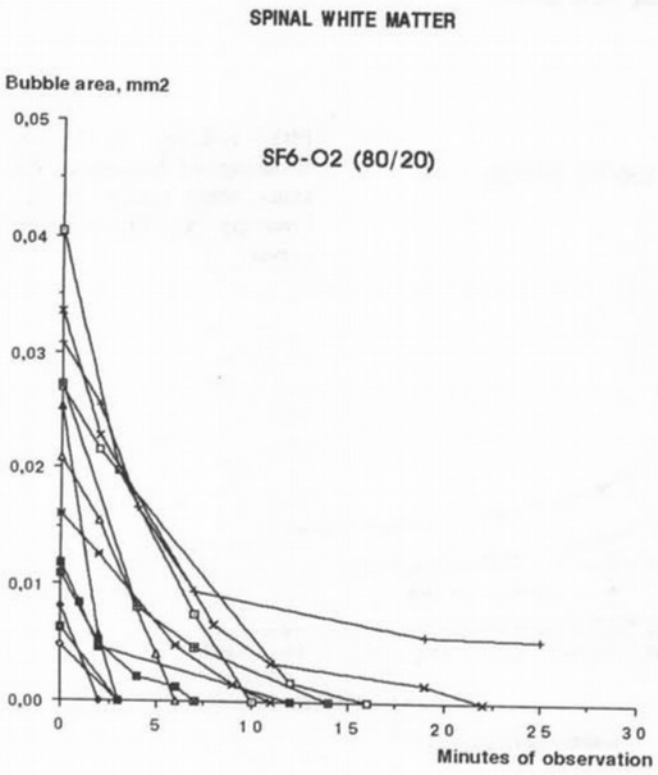

FIG. 7—Experiment B: Effect of SF_6–O_2 breathing of bubbles in spinal white matter. SF_6–O_2 breathing from first point on curves. No previous pressure exposure.

in the spinal white matter during SF_6–O_2 breathing, most bubbles would shrink and disappear (Figs. 6 and 7) faster than during air breathing. Sejrsen (13) has shown that countercurrent mechanisms exist in the brain and the same mechanism may be at work in the spinal cord. As in adipose tissue, the high solubility of SF_6 in the surrounding lipid tissue may initially cause most of the SF_6 to go into solution, little entering the bubble.

If the gas exchange between blood and bubble in a lipid tissue were limited by the extravascular diffusion, N_2 bubbles might grow during breathing of SF_6–O_2 due to the 1.6 times greater diffusibility (i.e., the product of diffusion coefficient and solubility coefficient) of SF_6 than of N_2 (Table 1). The present results do not support the idea of an extravascular diffusion-limited gas exchange since no growth of bubbles was observed during breathing of SF_6–O_2.

Although SF_6–O_2 breathing accelerates the disappearance of bubbles in certain tissues, it is hardly suitable in the treatment of DCS because some bubbles after an initial reduction become very stable, and a shift back to air breathing containing 79% N_2 would cause such bubbles to grow and remain in the tissues for a longer period (19,20). Further, SF_6 is a dense gas (6.50 g · liter^{-1}) (21) and will cause increased work of breathing, particularly during recompression. Finally, SF_6 is narcotic at increased pressures although it does not seem to produce any harmful effects during breathing at normobaric conditions (22).

The help of Associate Professor P. Sejrsen, Dr. med. sci. is gratefully acknowledged. The work was supported by grants from Fonden til Lægevidenskabens Fremme, AGA AB Medical Research Fund, The Laerdal Foundation for Acute Medicine, Novo Nordisk Fond, and Idrættens Forskningsråd.—*Manuscript received February 1995; accepted September 1995.*

Scanned for the Undersea and Hyperbaric Medical Society by The Rubicon Foundation
in cooperation with Global Underwater Explorers. (http://rubicon-foundation.org)

REFERENCES

1. Flynn ET, Catron PW, Bayne CG. Diving medical officer student guide. US Naval Technical Training Command 1981; (2-2).
2. Hills BA, Butler BD. The kangaroo rat as a model for type 1 decompression sickness. Undersea Biomed Res 1978; 5:309–321.
3. Gersh I, Hawkinson GE, Rathbun EM. Tissue and vascular bubbles after decompression from high pressure atmospheres, correlation of specific gravity with morphological changes. J Cell Comp Physiol 1944; 24:35–70.
4. Weathersby PK, Homer LD. Solubility of inert gasses in biological fluids and tissues: a review. Undersea Biomed Res 1980; 7:277–296.
5. Hyldegaard O, Madsen J. Influence of heliox, oxygen, and N_2O–O_2 breathing on N_2 bubbles in adipose tissue. Undersea Biomed Res 1989; 16:185–193.
6. Hyldegaard O, Møller M, Madsen J. Effect of He, O_2, and N_2O–O_2 breathing on injected bubbles in spinal white matter. Undersea Biomed Res 1991; 18:361–371.
7. Hyldegaard O, Madsen J. Effect of air, heliox, and oxygen breathing on air bubbles in aqueous tissues in the rat. Undersea Hyperbaric Med 1994; 21:413–424.
8. Armitage P, Berry GM. Statistical methods in medical research, 2d ed. Oxford, England: Blackwell Scientific Publications, 1987.
9. Kramer GY. Extensions of multiple range tests to group means with unequal numbers of replications. Biometrics 1956; 12:307–310.
10. Rafferty J, Norling R, McMath C, Tamaru R, Morganstein D. Statworks, version 1.1, Cricket Software. London: Heyden and Son Ltd. 1985;.
11. Sejrsen P. Convection and diffusion of inert gasses in cutaneous, subcutaneous, and skeletal muscle tissue. Capillary permeability, In: Crone C, Lassen NA, eds. Alfred Benzon Symposium II, Copenhagen: Munksgaard, 1970;586–596.
12. Sejrsen P, Tønnesen KH. Shunting by diffusion of inert gasses in skeletal muscle. Acta Physiol Scand 1972; 86:82–91.
13. Sejrsen P. Shunting by diffusion of gas in skeletal muscle and brain. Cardiovascular shunts. In: Johansen K, Burggren WW, eds. Alfred Benson symposium 21. Copenhagen: Munksgaard. 1985:452–466.
14. Piiper J, Meyer M. Diffusion–perfusion relationships in skeletal muscle: models and experimental evidence from inert gas washout. Adv Exp Med Biol 1984; 169:457–465.
15. Homer LD, Weathersby PK. How well mixed is inert gas in tissues? J Appl Physiol 1986; 60:2079–2088.
16. Homer LD, Weathersby PK, Survanshi S. How countercurrent blood flow and uneven perfusion affect the motion of inert gas. J Appl Physiol 1990; 69:162–170.
17. Tønnesen KH, Sejrsen P. Inert gas diffusion method for measurement of blood flow. Comparison of bolus method to directly measured blood flow in the isolated gastrocnemius muscle. Circ Res 1967; 20:552–564.
18. Hills BA. Intermittent flow in tendon capillary bundles. J Appl Physiol 1979; 46:696–702.
19. Thompson J. Kinetics of intraocular gases. Disappearance of air, sulfur hexafluoride, and perfluoropropane after pars plana vitrectomy. Ophtalmology 1989; 107:687–691.
20. Crittenden JJ, De Juan E Jr, Tiedeman J. Expansion of long-acting gas bubbles for intraocular use. Principles and practice. Arch Opthalmol 1985; 103:831–834.
21. Maio DA, Farhi LE. Effect of gas density on mechanics of breathing. J Appl Physiol 1967; 23:687–693.
22. Östlund A, Sporrung A, Linnarsson D, Lind F. Effects of sulfur hexafluoride on psychomotor performance. Clin Physiol 1992; 12:409–418.

Scanned for the Undersea and Hyperbaric Medical Society by The Rubicon Foundation
in cooperation with Global Underwater Explorers. (http://rubicon-foundation.org)

View publication stats